Journal of Materials Chemistry B

Accepted Manuscript

ROYAL SOCIETY OF CHEMISTRY

www.rsc.org/materialsB

Calcium Phosphate Nanocapsule Crowned Multiwalled Carbon Nanotubes For pH Triggered Intracellular Anticancer Drug Release

Shashwat S. Banerjee[a], Kiran J. Todkar[a], Ganesh V. Khutale[a], Govind P. Chate[b], Ankush V. Biradar[c], Manoj B. Gawande[d], Radek Zboril[d] and Jayant J. Khandare[b]*

[a]Actorius Innovations and Research, 100 NCL Innovation Park, Pune-411008, India.

[b]Maharashtra Institute of Pharmacy, Maharashtra Institute of Technology Campus, Kothrud, Pune-411038, India.

[c]Catalysis Division, CSIR-National Chemical Laboratory, Pune-411008, India.

[d]Regional Centre of Advanced Technologies and Materials, Faculty of Science, Department of Physical Chemistry, Palacky University, Šlechtitelů 11, 783 71, Olomouc, Czech Republic.

* All correspondence should be addressed to: jayant.khandare@mippune.edu.in

Abstract

We report calcium phosphate (CaP) nanocapsule crowned multiwalled carbon nanotube (CNT-GSH-G4-CaP) as a novel platform for intracellular delivery of an anticancer drug. As a *proof-of-concept*, CNT-GSH-G4-CaP demonstrates release of anticancer drug doxorubicin hydrochloride (DOX) within intracellular lysosomes from the interior cavity of CNT upon pH triggered CaP dissolution. Importantly, we found that the CNT with CaP nanolid can efficiently prevent untimely drug release at physiological pH but promotes DOX release at increased acidic milieu as observed in subcellular compartments such as lysosomes (~5.0). This "zero premature release" characteristic is of clinical significance in delivering cytotoxic drugs, by reducing systemic toxicity and thus beneficial for the effective anticancer treatment. We envision that this pH triggered CaP crowned CNT nanosystem would lead to a new generation of self-regulated platform for intracellular delivery of variety of anticancer drugs.

Keywords: carbon nanotube, calcium phosphate, nanocapsule, control release, cancer therapy

1. Introduction

In the past decade, design and development of effective nanoparticle-based drug delivery systems for treating cancer has been a top priority in biomedical sciences.[1-5] However, despite rapid advances, nanoparticle based chemotherapy is still a major challenge. For example, in many instances, the efficacy of the anticancer drug is hampered due to poor cellular internalization as well as insufficient intracellular drug release, limiting the dosages of anticancer drugs to the level below the therapeutic window.[6,7] Furthermore, one of the key requirements of such delivery systems is to enhance the efficacy of the delivered drug with fewer acute and chronic side effects.[4,8,9] To address this challenges, extensive research is being focused on the development of smart nanomedical platforms possessing two important prerequisites, "zero-premature release" and "stimuli responsive controlled release".[10] Towards this, stimuli-responsive capped mesoporous materials have demonstrated to be fascinating vehicles for the storage and controlled release of entrapped guests.[11-16] However, constructing a stimuli-responsive capped drug delivery system with control over the location and tuned drug release under physiological conditions remains a major challenge.[10,16] In this study, we report for the *first time* a smart pH-responsive calcium phosphate crowned CNT based nanosystem that facilitates the controlled release of anticancer drug doxorubicin hydrochloride (DOX), within acidifying intracellular compartments such as endosomes and lysosomes.

CNT's have attracted phenomenal interest as carriers of biologically relevant molecules.[17-20] The unique physicochemical and structural properties of these nanocarriers enable easy functionalization as well as offers benefit of integrating multiple diagnostic and therapeutic moieties on the same nanotube platform.[18,21,22] Furthermore, it is now established that CNT do

not require conjugation of antibodies or cell penetrating peptides for cellular internalization as their natural shape facilitates penetration across biological barriers.[19,23] Also, functionalized CNTs display low toxicity and non-immunogenicity,[24-26] as they are dispersible in water and compatible with biological fluids. Towards this directon we recently embarked on the feasibility of designing multicomponent conjugated fluorescent carbon nanotubes for intracellular trafficking and imaging performance by intelligent manipulation of their surface chemistry.[18]

Although various CNT based drug delivery or controlled release systems have been developed, in most of these systems, the bioactives to be delivered are attached through covalent or noncovalent binding to the CNT surface, leaving the inner cavity unutilized.[18,21,22,27] Here, we hypothesize that the loading of therapeutic drug in the inner cavity of CNT will provide the desired pharmacokinetics in anticancer drug delivery therapuetics. This is because the drug is protected from the physiological environment for its prelude bio-availibilty and selected release allows for lower drug loading through effective intracelluar site delivery. However, one of the major challenges in using CNTs as a nanoreservoir for drug delivery involves preventing the loaded drug from leaking out of CNTs.[28] Taking into account these challenges and being aware of the promising features of CNT as nanoreservoirs, we focused on the development of new tailor made pH-responsive CNT nanosystem. The key objective and concept used in this work involves use of calcium phosphate (CaP) nanocapsules as a symbiotic delivery system with CNT nanocarrier and for delivery gradient at cellular pH. In addition, CaP may act as a external capping agents in controlling the drug release. With motivation from our previous work, we sought to explore PAMAM-G4-NH_2 dendrimer templated CaP nanocapsules.[29] One of the advantages of using dendrimer as template is its nanoscale size and the 3-D spherical morphology which allows easy formation of CaP nanocapsules. Here, we envisioned that the

CaP nanocapsules will in addition offer the unique advantage of pH tunable properties. In the acidic environment the drug release can occur within the maturation process of endosomes into phasolysosomes. CaP nanocapsule will dissolve into nontoxic ions (calcium, phosphate ions) thus "triggers" for uncapping the pores resulting in uncapping of the CNT cavity and releasing the drug molecules as depicted in Fig. 1 A and B.

2. Experimental Section

2.1 Materials.

CNTs (outer diameter of 10-20 nm; length 10-30 μm; and purity > 95%) were purchased from J. K. Impex, Mumbai (India). PAMAM-G4-NH_2 (G4) dendrimer 10 wt% in methanol (Mw. 14214.7 Da, 64 end groups), 4-Dimethylaminopyridine (DMAP), 1-ethyl-3-(3-dimethylaminopropyl) carbodimide (EDC) HCl, Sephadex G10 were procured from Sigma-Aldrich (St. Louis, MO). Doxorubicin hydrochloride (DOX) was obtained from EMD Bioscience (Germany). Glutathione (GSH) was procured from Sigma-Aldrich Chemical Co. Germany. Calcium chloride dehydrate ($CaCl_2$ $2H_2O$) was procured from Merck (India). Disodium hydrogen phosphate (Na_2HPO_4) was purchased from Rankem (India). HCT116 cells were procured from National Centre for Cell Science, Pune, India. McCoy's5A and fetal bovine serum (FBS) were procured from Life Technologies, USA. Penicillin and streptomycin were purchased from Sigma-Aldrich, USA. LysoTracker® Green DND-26 was purchased from Invitrogen, USA. Ultrapure water (MilliQ) acquired from a Synergy UV® water purification system (Merck Millipore, Germany) was used throughout. All other chemicals were of analytical grade and used without further purification.

2.2 Synthesis of PAMAM G4-GSH (G4-GSH)

50 mg of PAMAM-G4-NH_2 (G4) was added to 69 mg of glutathione (GSH) dissolved in a sufficient quantity of MilliQ water in presence of EDC.HCl and DMAP as catalysts at pH ~ 6.0. The reaction was carried out at room temperature with continuous stirring for 24 h. The conjugate was purified by size exclusion process using Sephadex G-10 column to remove the unreacted GSH**.**

2.3 Synthesis of CNT-G4-GSH

First, CNT was purified and oxidized using a modified literature procedure.[18,30] To synthesize CNT-G4-GSH conjugate, 2.5 mg of functionalized CNT was sonicated in the presence of *N*-(3-dimethylaminopropyl)-*Ń*-ethylcarbodiimide hydrochloride (EDC.HCl) at pH ~ 6.0 for 30 min at room temperature. 100 mg of G4-GSH was then added to the CNT solution. The reaction was continuously stirred for 24 h at room temperature on a magnetic stirrer. The modified CNT was collected and washed with MilliQ water by ultra centrifugation to remove unbound G4-GSH, then dried at room temperature to obtain CNT-G4-GSH.

2.4 Loading of doxorubicin hydrochloride (DOX)

CNT-G4-GSH (3.2 mg) were added to 1.0 mg/mL solution of DOX in water, and the resulted mixture was sonicated for 4 h to let the DOX solution enter the inner cavity of CNTs.

2.5 Calcium phosphate (CaP) mineralization of polymer

In this reaction, the resulting DOX loaded CNT-G4-GSH was mixed with $CaCl_2$ (1.0 mL, 40 mM) and stirred overnight at room temperature. Na_2HPO_4 (1.0 mL, 40 mM) was then added to

the solution containing CNT-G4-GSH/$CaCl_2$. The pH of the solution was adjusted to 8.0 with 0.1N NaOH and stirred for 24 h at room temperature. The CNT-G4-GSH-CaP core shell nanocapsule was collected and washed with MilliQ water by ultracentrifugation, then collected and dried at room temperature. The concentration of DOX remaining in the supernatant solution was determined spectrophotometrically at λ_{max} of 480 nm.

2.6 Characterization

TEM analysis was carried out using Tecnai FEI G2, using an accelerating voltage of 200 kV. The samples were obtained by placing a drop of sample dispersed in isopropyl alcohol (IPA) and deposited on a coated 200 mesh Copper grid and evaporated in air at room temperature. Microscopic images were obtained by HRTEM TITAN 60-300 with X-FEG type emission gun, operating at 80 kV. This microscope is equipped with Cs image corrector and a STEM high-angle annular dark-field detector (HAADF). The point resolution is 0.06 nm in TEM mode. The elemental mappings were obtained by STEM-Energy Dispersive X-ray Spectroscopy (EDS) with acquisition time 20 min. For HRTEM analyses, the powder samples were dispersed in Isopropanol and 5 min ultrasonicated. One drop of this solution was placed on a copper grid with holey carbon film. The sample was dried at room temperature. FTIR spectral studies were carried out using a Bruker Tensor 37 attenuated total reflectance-fourier transform infrared spectroscopy (ATR-FTIR) spectrometer in the range between 2000 and 400 cm^{-1}, with a resolution of 2 cm^{-1}.The hydrodynamic diameter was determined using dynamic light scattering (DLS). Measurements were carried out at room temperature on a NanoBrook 90Plus particle size analyzer instrument. The UV-vis absorption spectra were recorded on a labIndia UV-3000^{+}

spectrometer. Fluorescence study was carried out using Jasco spectrofluorometer FP-8300 in the range between 500 and 700 cm^{-1} at an excitation wavelength of 480 nm.

2.7 *In vitro* dissolution studies

The profile for the *in vitro* release of DOX from CNT-G4-GSH-CaP-DOX nanocapsules were established by suspending the nanocapsules in 20 ml of phosphate buffer with different pH values of 7.4 and 5.0. Release samples were withdrawn at different time intervals, centrifuged and clear liquid aliquot were taken for the analysis. The amount of DOX released from the nanocapsules were analysed by UV spectroscopy at λ_{max} of 480 nm. In order to evaluate the amount of DOX encapsulated, CNT-G4-GSH-CaP-DOX was incubated in phosphate buffer of pH 5 for 5 min, then in pH 7 and again in pH 5.0 to determine the DOX release from surface and from the cavity of CNT.

2.8 Cell culture

HCT116 was procured from NCCS and cultured in McCoy's 5A, supplemented with 10% fetal bovine serum and 100 unit mL^{-1} penicillin, 100 μg mL^{-1} streptomycin.

2.9 Time dependent cellular entry studies using fluorescence microscopy

HCT116 cells were plated at 2 x$10^5$$mL^{-1}$ on cover slips in 35 mm culture dishes. After 24 h, cells were treated with free DOX and CNT-GSH-G4-CaP-DOX nanosystem in a time dependent manner (4 h and 48 h). The concentration of DOX was 17.2 μM. Cover slips were removed after consecutive time points and processed for fluorescence microscopy. Cells were fixed with 2.0% paraformaldehyde for 15 min at room temperature followed by permeabilization with 0.1%

Triton X-100 in phosphate buffered saline (PBS) for 5 min. Cells were then washed three times in PBS and cover slips were mounted in ultracruz mounting media with 4′-6-diamidino-2-phenylindole (DAPI) (Santa Cruz) and examined under fluorescence microscope (Leica DM2500 M, Germany).

2.10 Cell viability assay

Cytotoxic activity of compounds was quantitatively determined by a colorimetric assay utilizing (3-(4,5-Dimethylthiazol-2-yl)-2,5-diphenyltetrazolium bromide) (MTT), as described previously.[31] Briefly, HCT116 cells were seeded at 3000 cells/well in 96-well plates and maintained in culture for 24 h at 37 ^{o}C in McCoy's 5A medium supplemented with 10% FBS. The free DOX and CNT-GSH-G4-CaP-DOX nanosystemwere added in the wells and incubated for 48 h. DOX concentration in the study was 1.06 mM. The cells were then incubated with MTT for 3 h at 37 ^{o}C. The MTT was reduced to an insoluble formazan precipitate by mitochondrial succinic dehydrogenase of the viable cells. After removal of the media, dimethyl sulfoxide (DMSO) solution was added to each well. After complete solubilization of the dark blue crystal of MTT formazan, the absorbance of the content of each well was measured at 570 nm with microplate reader on Infinite® F200 PRO (Tecan, Austria). Background readings (blank) were obtained from cell-free wells containing media also incubated with the MTT solution.

3. Results and discussion

3.1 Synthesis and characterization of CNT-G4-GSH-CaP-DOX

We followed a multi-step process (Fig.2) to synthesize the CNT-G4-GSH-CaP-DOX nanosystem. CNT's were first subjected to oxidation treatment to eliminate the contaminants and

concomitantly generate abundant carboxylic groups at the tips and defect sites of CNT surfaces according to a modified literature procedure.[18,30] Furthermore, the oxidation of CNT results in breaking of sp^2 backbone carbons and leads to formation of various (C=O, COOH or C-O-C) functional groups on to the CNT surface. Furthermore, the treatment was expected to impart severe etching of the carbon allotrope surfaces (both outer and inner) of the CNTs, resulting in tubes of shorter length with opened ends.[30] As the treated CNTs have open ends and their exterior and interior surfaces are both hydrophilic, it is expected that aqueous solutions containing drug can flow into the inner cavity of CNTs, especially with the help of sonication. Conversely, in a separate reaction PAMAM G4-NH_2 was conjugated with GSH by 1-ethyl-3-(3-dimethylaminopropyl) carbodimide (EDC).HCl coupling method (Fig. 2). An amide linkage was formed between the carboxylic-group of GSH and amine group of G4. G4-GSH was then grafted with the functionalized CNT by EDC coupling reaction between the amine groups of GSH and the carboxyl groups of the CNT-COOH. Then using a method that we previously reported (see experimental section), CaP nanocapsules were synthesized using the dendrimers conjugated at the open CNT tips as the gatekeepers for DOX molecules.[29] The encapsulation efficiency of DOX in CNT-GSH-G4-CaP-DOX was found to be 385 mg • g^{-1} (an average of $n = 3$ batches).

The CNT-G4-GSH-CaP-DOX nanosystem was characterized by transmission electron microscopy (TEM). Fig. 3 A and B shows the TEM micrograph of CNT-G4-GSH-CaP-DOX and CNT-G4-GSH-DOX without CaP. From the TEM micrographs we could observe spherical CaP crystal developed at the open tip ends of CNT (Fig. 2 B) in CNT-G4-GSH-CaP-DOX nanosystem. The reason for formation of CaP at the tip is because of the presence of the conjugated G4-GSH which favors nucleation of CaP on the surface to produce mineralized CaP shell (Fig. 2 A, B). The hydrodynamic size and PDI of CNT-G4-GSH-CaP-DOX were analyzed

to be 529 ±13.6 nm and 0.184 ±0.088, respectively. Fig. 3 C shows characteristic colored solution of well dispersed CNT-G4-GSH-CaP-DOX in aqueous media. The higher dispersibility in aqueous media resulted from the presence of PAMAM G4 dendrimers and CaP nanocapsules chemically conjugated to CNTs containing carboxylic groups.

To confirm encapsulation of DOX in the cavity of CNT and complex structure of nanocarrier high angle annular dark-field scanning transmission electron microscopy (HAADF-STEM) images and STEM-Energy Dispersive X-ray Spectroscopy (EDS) profiling of CNT-G4-GSH-CaP-DOX was done (Fig. 4A). The results clearly indicate the presence of all involved important species such as C, Ca, P, and N from corresponding moieties (Fig. 4B). As depicted in Fig. 2, the presence of DOX, PAMAM G4-NH_2, and CaP, was confirmed by HAADF-STEM images (Fig. 4B. In particular, at the end of CNT, the swelling part of nanotube with increased amounts of Ca and O confirms the presence of CaP capping agent. The increased concentration of nitrogen at the end of nanotube is expected due to PAMAM G4-NH_2. Importantly, nitrogen is distributed inside the CNT, which reflects the encapsulation of DOX, although some fraction of DOX on the outer surface of the nanotube also cannot be excluded. To further confirm DOX encapsulation, the amount of DOX present on the CNT surface and cavity was determined. The study revealed presence of ~20% DOX on the surface and ~80% in the CNT cavity, thus confirming significant encapsulation of DOX.

The nanosystem was characterized by ATR-FTIR to verify the successful covalent conjugation of G4-GSH to functionalized CNT and formation of CaP nanocapsules on CNT. Fig. 5shows the FT-IR spectra of oxidized CNT, CNT-G4-GSH and CNT-G4-GSH-CaP-DOX respectively. IR spectrum of CNT showed characteristic peak of carbonyl group at 1635 cm^{-1} which confirmed the formation of carboxyl groups during the acid-oxidated process on the ends

and defect sites on the sidewall.[18] The presence of a large number of carboxyl groups on CNT is important for conjugation of other components. The FT-IR spectrum of CNT-G4-GSH showed new peaks at 1578 cm^{-1} and 1703 cm^{-1} corresponding to N-H deformation and amide bonds linking G4-GSH to the CNT. Therefore, we could infer conjugation of G4-GSH to CNT. Further, the FT-IR spectrum of CNT-G4-GSH-CaP-DOX showed characteristic absorption bands of the apatite phase at 511 and 596 cm^{-1} due to P-O-P bending vibration (υ_4). The presence of DOX was also confirmed FT-IR analysis. The IR spectrum of free DOX showed multiple bands at 969, 1072, and 1094 cm^{-1} due to the different quinone and ketone carbonyls of DOX. The spectrum of CNT-G4-CaP loaded with DOX showed new peaks at 1076, and 1203 cm^{-1} which might be due to the presence of DOX. Thus, the FT-IR analysis indicates that DOX is indeed loaded into CNT-G4-CaP. In addition, DOX loading on CNT-GSH-G4-CaP-DOX was also confirmed by fluorescence spectroscopy. As shown in Fig. 6, DOX in water displays λ_{em} at ~ 560 nm. The spectrum of CNT-GSH-G4-CaP-DOX incubated in water also displayed the typical absorption band from DOX indicating loading of DOX.UV–Vis spectroscopy also corroborated the presence of DOX in CNT-GSH-G4-CaP-DOX. As shown in the inset of Fig. 6, the spectrum of DOX and CNT-GSH-G4-CaP-DOX solutions show typical absorption at ~ 480 nm, indicating the presence of DOX.

3.2 *In vitro* release study

As an initial assessment to verify the effectiveness of CNT-GSH-G4-CaP-DOX for pH-controlled DOX release, we employed pH variation between physiological pH (pH 7.4) and the low pH condition (pH 5.0). Fig. 7A shows the DOX release profiles from CNT-GSH-G4-CaP-DOX at pH 7.4 and at pH 5.0. There was low release of DOX from CNT-GSH-G4-CaP-DOX at

pH 7.4. This is because at higher pH solubility of CaP is low and hence the CNT end blockers were maintained thus hindering DOX release at physiological pH values. The observed DOX release probably stemmed from loosely surface bound DOX. Conversely, at pH 5.0, ~ 77% DOX were released from the nanosystem by 48 h due to dissolution of blockers resulting in uncapping of CNT open ends thereby triggering DOX release. The pH-dependent dissolution of CaP-like materials has already been confirmed in our earlier work.[32] We have shown that at physiological pH condition CaP dissolution was low. However, when the pH was lowered to 5.0, the amount of Ca^{2+} released due to CaP dissolution was almost three times higher than that released at pH 7.4 after 72 h.[32] To confirm the capping efficiency, release of DOX from CNT-GSH-G4-DOX without CaP blocker was examined at pH 7.4 and 5.0. CNT-GSH-G4-DOX exhibited fast DOX release profile irrespective of the pH value of the release medium (Fig. 7B). This is because, CNT-GSH-G4-DOX has open pores and lacks the pore-blocking species; thus it could not prevent DOX release at physiological pH values. The result indicates successful symbiotic drug delivery strategy with higher efficiency. This pH-sensitive release behaviour is of particular interest as it can reduce premature drug release during circulation but specifically enhance intracellular drug release, which will be definitely beneficial to effective cancer treatment.

3.3 *In vitro* fluorescence imaging

The feasibility of using the CNT-GSH-G4-CaP-DOX nanosystem for intracellular drug delivery was studied using human colon epithelial HCT116 cells. As the CNT-GSH-G4-CaP-DOX nanosystem are taken up by the cells and trafficked into the early endosomes and then into the late endosomes/lysosomes, the nanosystems were expected to experience an increasingly acidic

environment. After incubation of HCT116 cells with DOX and CNT-GSH-G4-CaP-DOX for 4 h, nanosystems were found to internalize into the cells and predominantly localized in LysoTracker labeled (green fluorescence) acidic organelles, as indicated by bright orange fluorescence owing to merging of the green (LysoTracker) and red (DOX) fluorescence (Fig.8(a)). The cellular uptake of CNT-GSH-G4-CaP-DOX is mainly due to its shape. Our recent studies have also demonstrated the significant impact of CNT shape on the cell dynamics.[19]

Because of their tubular shape, CNTs creates snaking effect which promote penetration of membranes, uptake by cells, and strong interactions with various protein systems.[8] The intracellular release of DOX was attributed to the decomposition of CaP nanocapsules in the acidic lysosomal compartments, consistent with previous reports of the dissolution of CaP because of the acidity of the lysosomes. This finding is consistent with the DOX release patterns from CNT-GSH-G4-CaP-DOX at pH 5.0 (Fig. 7A). In contrast, cells treated with free DOX showed red fluorescence mainly in the cell nuclei.

At 48 h, most of the DOX resided in the nuclei for cells treated with CNT-GSH-G4-CaP-DOX, suggesting the efficient release of DOX from CNT-GSH-G4-CaP-DOX (Fig. 8(b)). The subcellular distributions of DOX from CNT-GSH-G4-CaP nanosystem indicate pH-triggered DOX release after the CaP nanocapsules dissolve. Based on *in vitro* results, we confirmed that the CaP nanocapsule is effective in preventing DOX release from CNT-GSH-G4-CaP-DOX before endocytosis, and the DOX release can be facilitated within lysosomes by the dissolution of CaP nanocapsule.

3.4 Cell viability study

The ability of CNT-GSH-G4-CaP-DOX nanosystem as cellular viability was studied by MTT assay. The *in vitro* cytotoxicity of CNT-GSH-G4-CaP-DOX was examined on HCT116 cells (Fig. 9). We thus incubated HCT116 cells in the culture medium with CNT-GSH-G4-CaP, CNT-GSH-G4-DOX, CNT-GSH-G4-CaP-DOX and free DOX, which served as the control, for 48 h. At 48 h, both CNT-GSH-G4-DOX, CNT-GSH-G4-CaP-DOX nanosystems nanotubes exhibited toxicity as free DOX in HCT116 cells. Based on these results, it can be summarized that CNT-GSH-G4-CaP-DOX platform possess the tailor-made pH-sensitive gated feature.

4. Conclusion

In summary, we have designed a CNT based nanosystem crowned with inorganic CaP nanocapsule which is capable of releasing guest drug under pH control. The CaP nanocapsule act as adjucnt nanocarrier and simultaneoulsy a gatekeeper to prevent the encapsulated anticancer drug DOX from escaping under extracellular conditions, whereas they can be dissolved within the lysosomal compartments, where the pH value is near 5.0. Furthermore, the CaP crowned nanocarrier with DOX loaded in their inner cavity will not only increase the amount of drug loading and its release from the system, but also provides a linear and sustainable drug release profile. We envision that the finely tuned tailor-made pH triggered delivery achieved in these systems would lead to a new generation of carrier materials for intracellular delivery of a variety of anticancer drugs.

Acknowledgment

Authors would like to acknowledge financial support from the Biotechnology Ignition Grant (BIG), Biotechnology Industry Research Assistance Council (BIRAC) and Department of Biotechnology (DBT) India. The authors gratefully acknowledge the support by the project LO1305 of the Ministry of Education, Youth and Sports of the Czech Republic. Authors are thankful to Dr. Klara Safarova for HRTEM images.

References

1. D. Peer, J. M. Karp, S. Hong, O. C. Farokhzad, R. Margalit and R. Langer, *Nat Nanotechnol*, 2007, **2**, 751-760.
2. I. L. Medintz, H. T. Uyeda, E. R. Goldman and H. Mattoussi, *Nat Mater*, 2005, **4**, 435-446.
3. J. M. Nam, C. S. Thaxton and C. A. Mirkin, *Science*, 2003, **301**, 1884-1886.
4. S. S. Banerjee and D. H. Chen, *Nanotechnology*, 2008, **19**, 265602.
5. S. S. Banerjee, A. Jalota-Badhwar, S. D. Satavalekar, S. G. Bhansali, N. D. Aher, R. R. Mascarenhas, D. Paul, S. Sharma and J. J. Khandare, *Adv Healthc Mater*, 2013, **2**, 800-805.
6. K. Ulbrich and V. Subr, *Adv Drug Deliv Rev*, 2004, **56**, 1023-1050.
7. J. Z. Du, X. J. Du, C. Q. Mao and J. Wang, *J Am Chem Soc*, 2011, **133**, 17560-17563.
8. J. Kaiser, *Science*, 2009, **326**, 218-220.
9. T. Tsuruo, M. Naito, A. Tomida, N. Fujita, T. Mashima, H. Sakamoto and N. Haga, *Cancer Sci*, 2003, **94**, 15-21.
10. J. L. Vivero-Escoto, Slowing, II, C. W. Wu and V. S. Lin, *J Am Chem Soc*, 2009, **131**, 3462-3463.
11. A. B. Descalzo, R. Martinez-Manez, F. Sancenon, K. Hoffmann and K. Rurack, *Angew Chem Int Ed Engl*, 2006, **45**, 5924-5948.
12. B. G. Trewyn, Slowing, II, S. Giri, H. T. Chen and V. S. Lin, *Acc Chem Res*, 2007, **40**, 846-853.
13. Slowing, II, J. L. Vivero-Escoto, C. W. Wu and V. S. Lin, *Adv Drug Deliv Rev*, 2008, **60**, 1278-1288.
14. K. K. Coti, M. E. Belowich, M. Liong, M. W. Ambrogio, Y. A. Lau, H. A. Khatib, J. I. Zink, N. M. Khashab and J. F. Stoddart, *Nanoscale*, 2009, **1**, 16-39.
15. E. Aznar, L. Mondragon, J. V. Ros-Lis, F. Sancenon, M. D. Marcos, R. Martinez-Manez, J. Soto, E. Perez-Paya and P. Amoros, *Angew Chem Int Ed Engl*, 2011, **50**, 11172-11175.

16. H. P. Rim, K. H. Min, H. J. Lee, S. Y. Jeong and S. C. Lee, *Angew Chem Int Ed Engl*, 2011, **50**, 8853-8857.
17. Z. Liu, W. Cai, L. He, N. Nakayama, K. Chen, X. Sun, X. Chen and H. Dai, *Nat Nanotechnol*, 2007, **2**, 47-52.
18. J. J. Khandare, A. Jalota-Badhwar, S. D. Satavalekar, S. G. Bhansali, N. D. Aher, F. Kharas and S. S. Banerjee, *Nanoscale*, 2012, **4**, 837-844.
19. S. S. Banerjee, A. Jalota-Badhwar, P. Wate, S. Asai, K. R. Zope, R. Mascarenhas, D. Bhatia and J. Khandare, *Biomaterials Science*, 2014, **2**, 57-66.
20. K. Kostarelos, L. Lacerda, G. Pastorin, W. Wu, S. Wieckowski, J. Luangsivilay, S. Godefroy, D. Pantarotto, J. P. Briand, S. Muller, M. Prato and A. Bianco, *Nat Nanotechnol*, 2007, **2**, 108-113.
21. D. Tasis, N. Tagmatarchis, A. Bianco and M. Prato, *Chem Rev*, 2006, **106**, 1105-1136.
22. M. Das, R. P. Singh, S. R. Datir and S. Jain, *Mol Pharm*, 2013, **10**, 3404-3416.
23. Z. Liu, X. Li, S. M. Tabakman, K. Jiang, S. Fan and H. Dai, *J Am Chem Soc*, 2008, **130**, 13540-13541.
24. H. Dumortier, S. Lacotte, G. Pastorin, R. Marega, W. Wu, D. Bonifazi, J. P. Briand, M. Prato, S. Muller and A. Bianco, *Nano Lett*, 2006, **6**, 1522-1528.
25. E. Heister, C. Lamprecht, V. Neves, C. Tilmaciu, L. Datas, E. Flahaut, B. Soula, P. Hinterdorfer, H. M. Coley, S. R. Silva and J. McFadden, *ACS Nano*, 2010, **4**, 2615-2626.
26. C. M. Sayes, F. Liang, J. L. Hudson, J. Mendez, W. Guo, J. M. Beach, V. C. Moore, C. D. Doyle, J. L. West, W. E. Billups, K. D. Ausman and V. L. Colvin, *Toxicol Lett*, 2006, **161**, 135-142.
27. Z. Liu, X. Sun, N. Nakayama-Ratchford and H. Dai, *ACS Nano*, 2007, **1**, 50-56.
28. X. Luo, C. Matranga, S. Tan, N. Alba and X. T. Cui, *Biomaterials*, 2011, **32**, 6316-6323.
29. J. J. Khandare, A. Jalota-Badhwar, N. Taneja, R. R. Mascarenhas, K. Vadodaria, K. R. Zope and S. S. Banerjee, *Partcle and Particle Systems Chatacterization*, 2013, **30**, 494-500.
30. *United States Pat.,* 2010.
31. A. O. Lobo, E. F. Antunes, A. H. A. Machado, C. Pacheco-Soares, V. J. Trava-Airoldi and E. J. Corat, *Materials Science and Engineering: C*, 2008, **28**, 264-269.
32. S. S. Banerjee, M. Roy and S. Bose, *Advanced Enginnering Materials*, 2011, **13**, B10-B17.

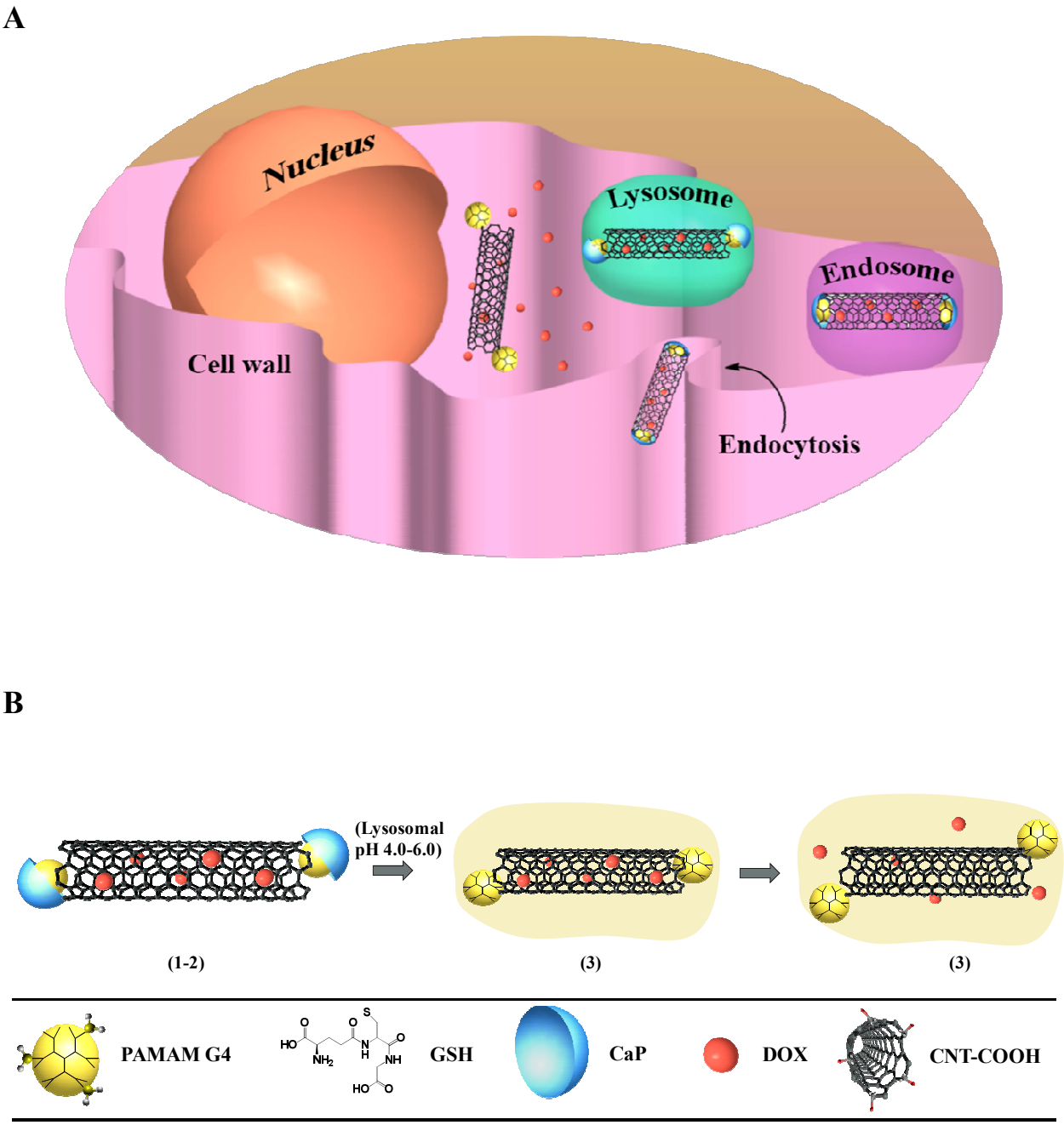

Fig. 1. (A, B) Schematic illustration of DOX-loaded CaP nanocapsule gated CNT based nanosystem and triggered drug release under intracellular endo/lysosomal conditions; (C) Synthesis scheme of the DOX loaded CNT-G4-GSH-CaP nano gate.

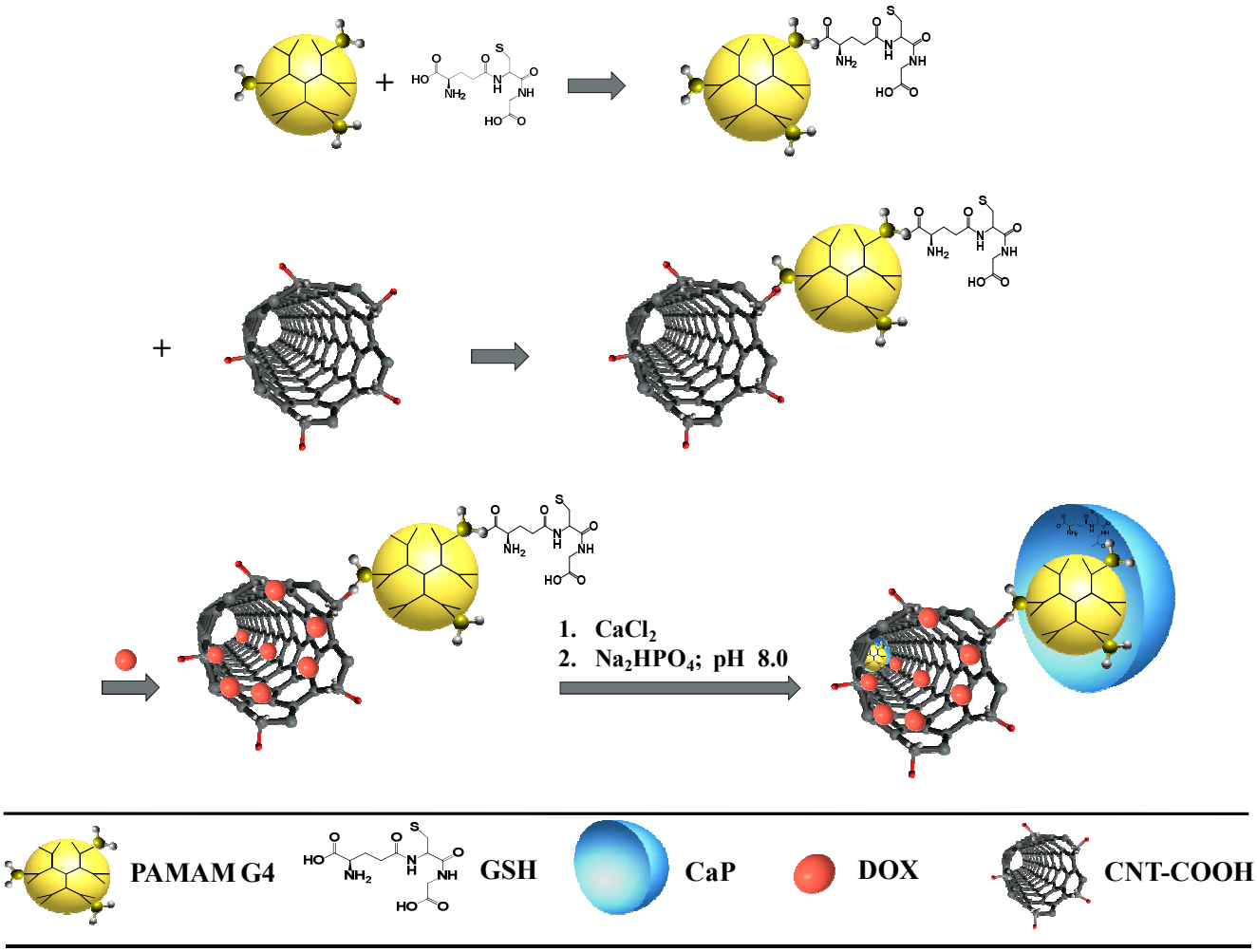

Fig. 2. Synthesis scheme of the DOX loaded CNT-G4-GSH-CaP nanosystem.

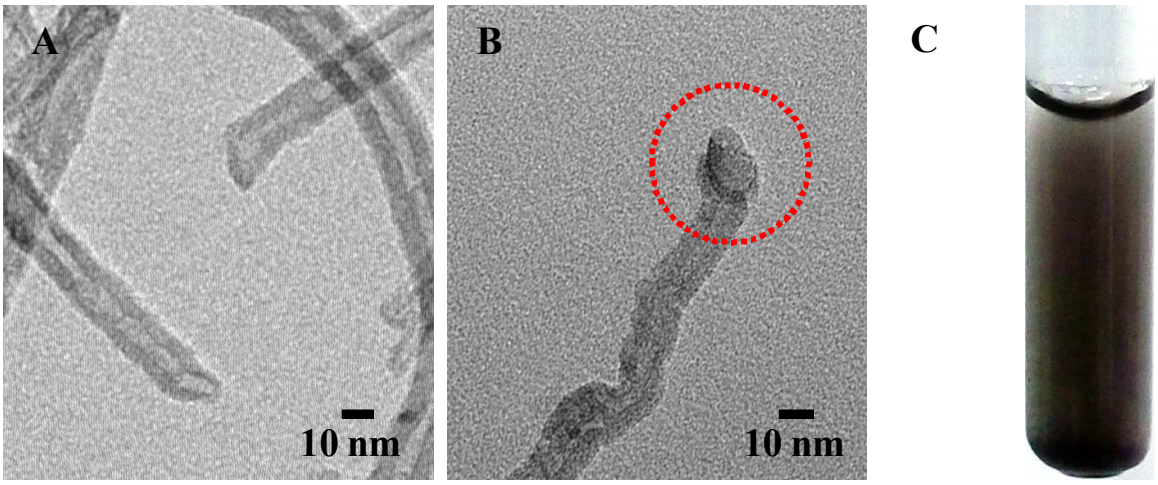

Fig. 3. TEM micrographs of (A) CNT-GSH-G4-DOX. (B) CNT-GSH-G4-CaP-DOX; the CNT type structure is clearly visualized with the CaP nanogate (circled in red) at the end. (C) Aqueous dispersibility of CNT-GSH-G4-CaP-DOX due to surface functionalization and the presence of G4 dendrimer and CaP nanocapsule.

A

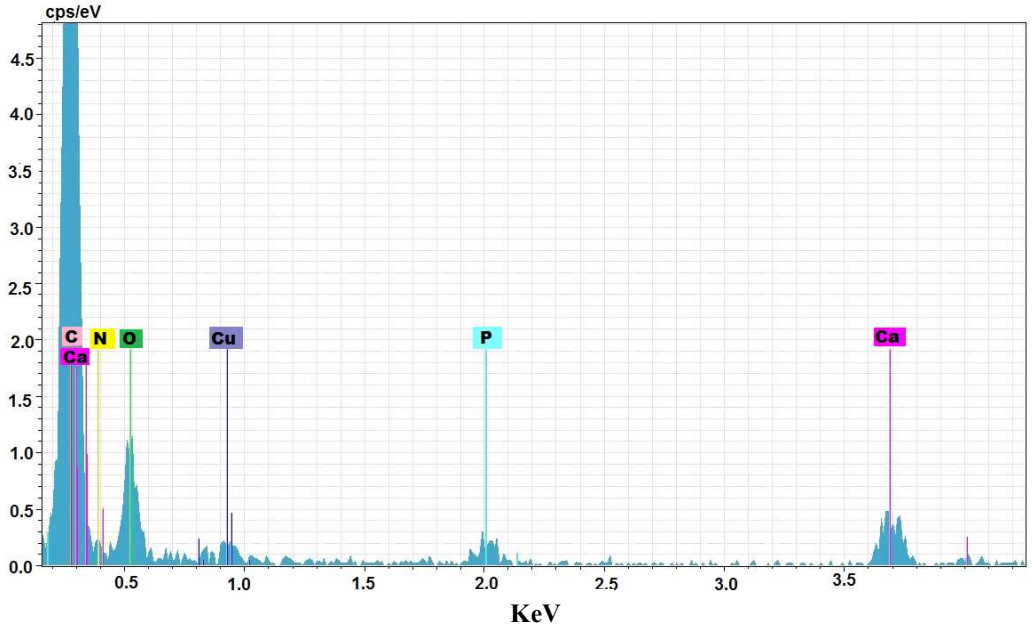

B

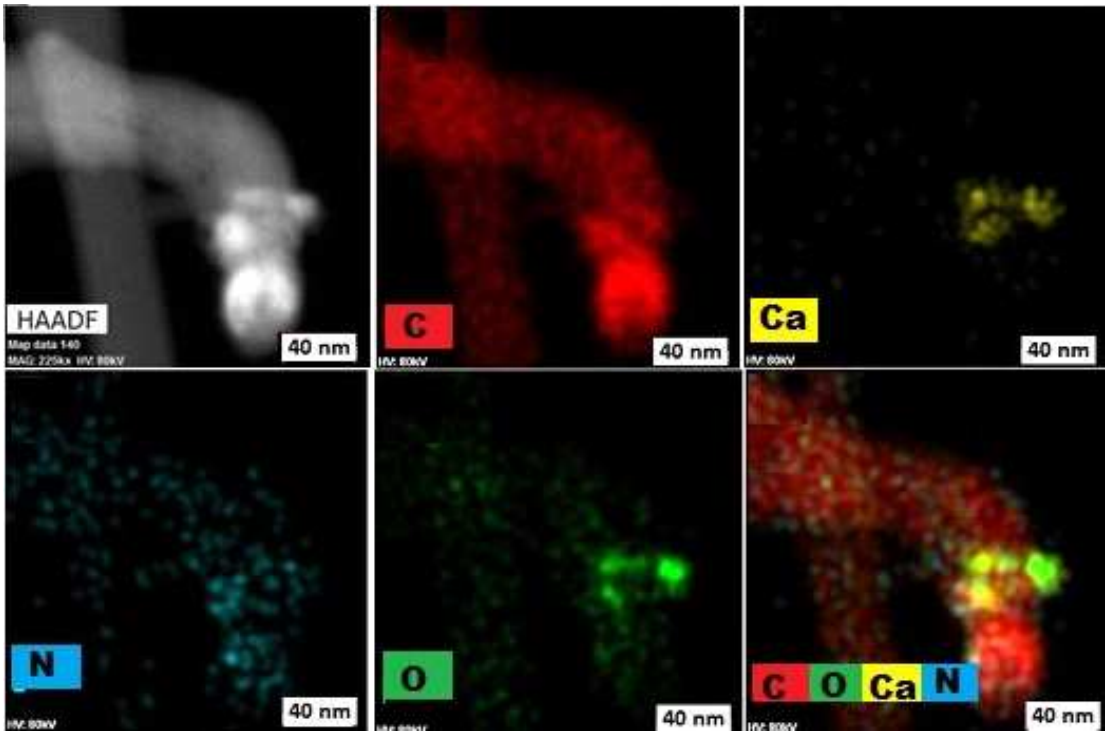

Fig. 4. (A) STEM-Energy Dispersive X-ray Spectroscopy (EDS) spectrum of CNT-G4-GSH-CaP-DOX showing carbon, calcium, nitrogen, oxygen, and phosphorus (copper peak is from copper grid, which should be excluded). (B) High angle annular dark-field scanning transmission electron microscopy (HAADF-STEM) of CNT-G4-GSH-CaP-DOX with corresponding elemental maps.

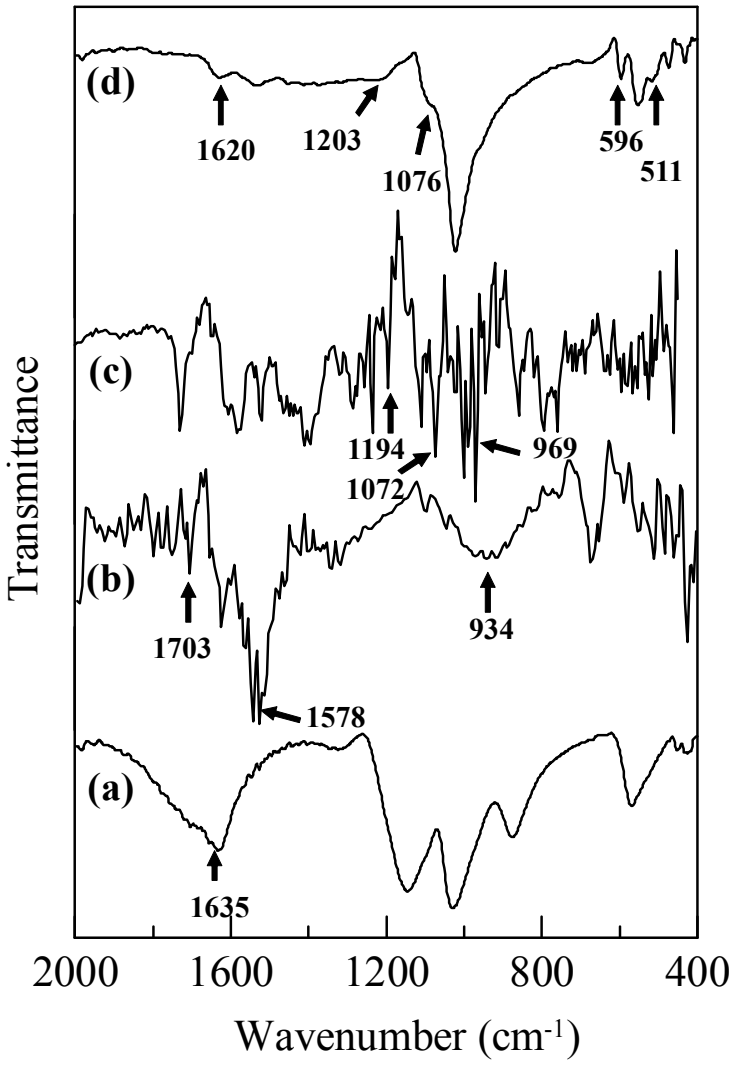

Fig. 5. FT-IR spectra of (a) CNT, (b) CNT-G4-GSH, (c) DOX and (d) CNT-G4-GSH-CaP-DOX.

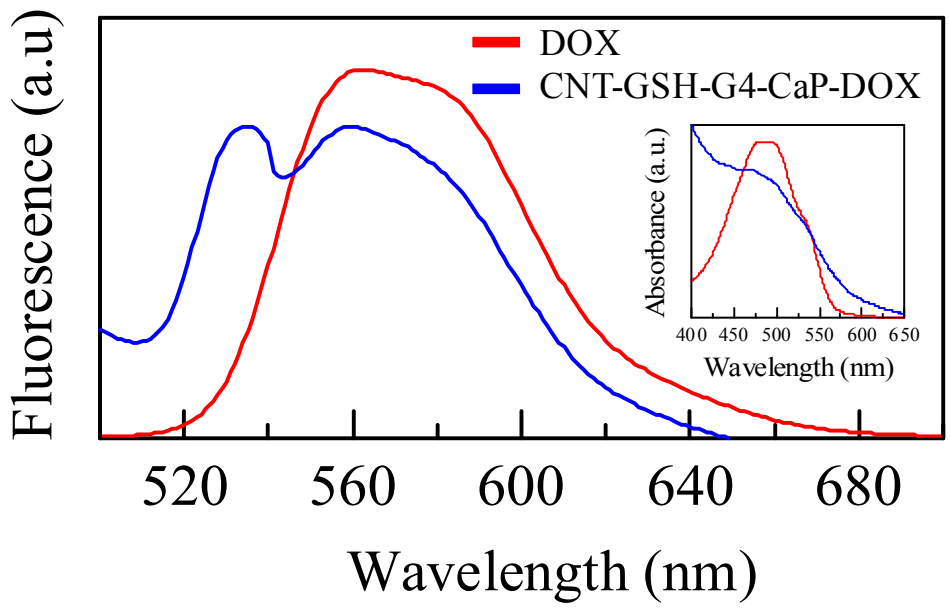

Fig. 6. Fluorescence spectra of DOX and CNT-G4-GSH-CaP-DOXat an excitation wavelength of 480 nm.The inset shows UV-Vis spectra of DOX and CNT-G4-GSH-CaP-DOX.

A

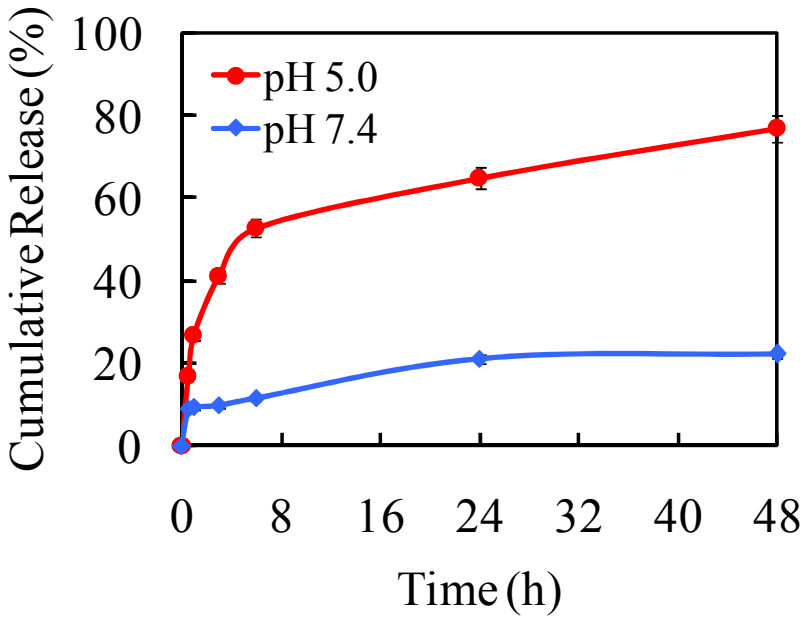

B

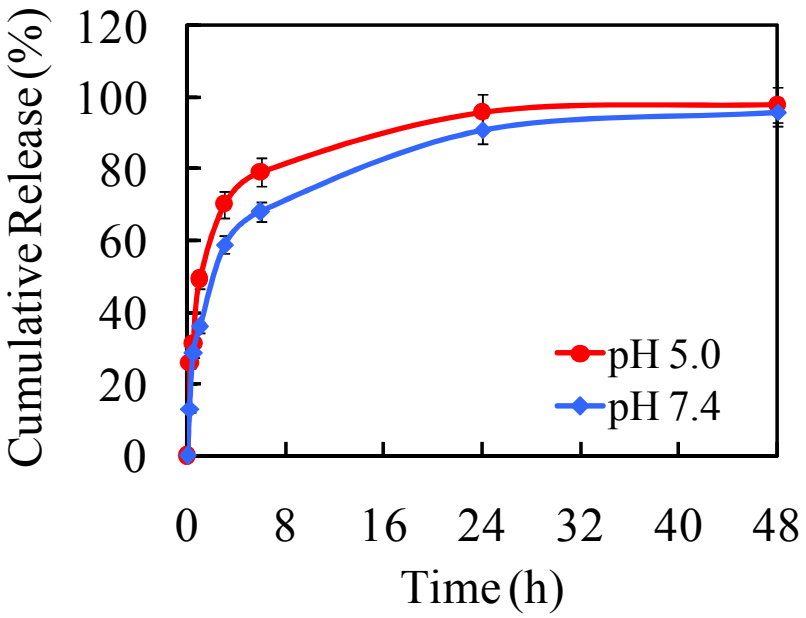

Fig. 7. Time dependent cumulative release of DOX from (A) CNT-G4-GSH-CaP-DOX and (B) CNT-G4-GSH-DOX without CaP blockers at different pH values.

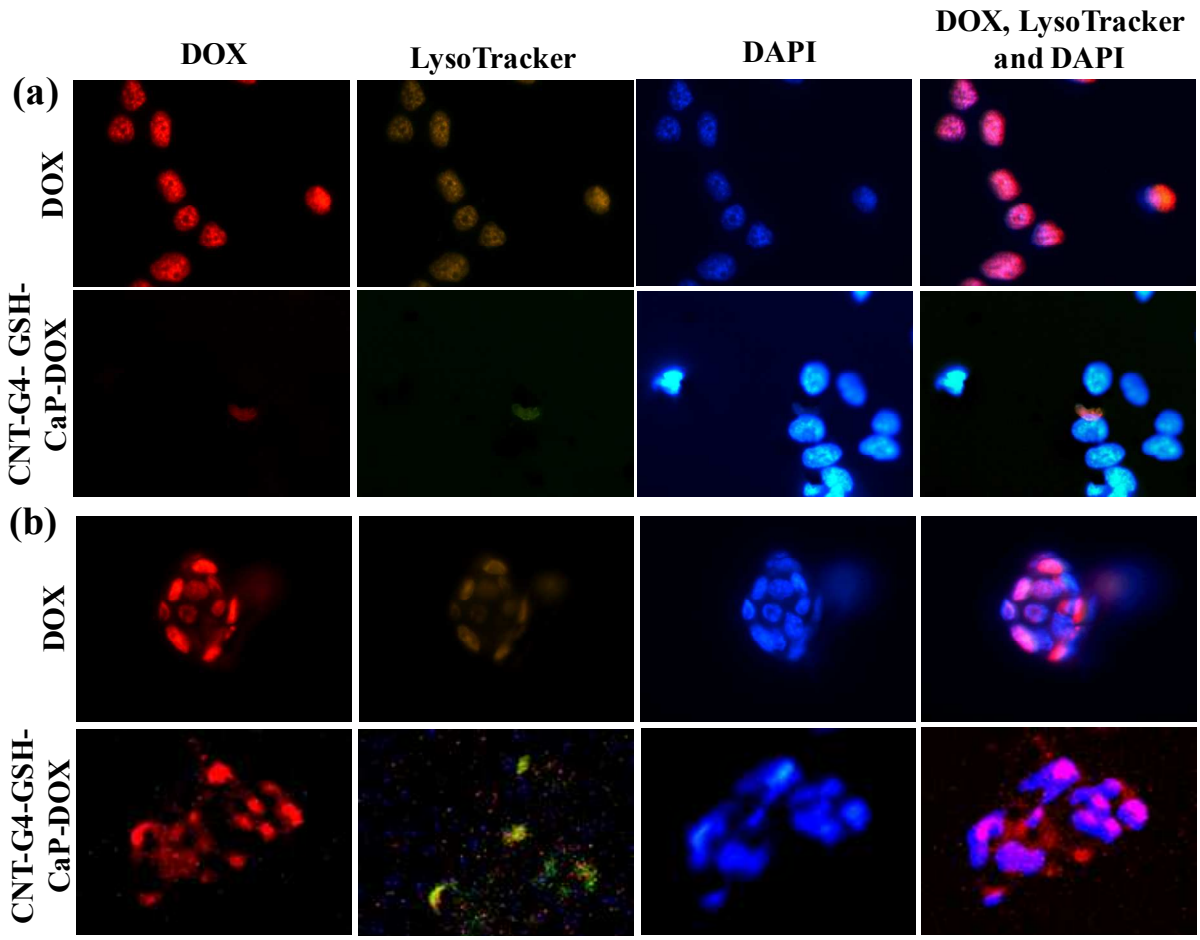

Fig. 8. Fluorescence images of HCT116 cells treated with LysoTracker (50 nM), free DOX, CNT-G4-GSH-CaP-DOX. Green fluorescence is associated with LysoTracker, the red fluorescence is expressed by free DOX, released DOX. (a) At 4 h exposure, the intracellular release of DOX was attributed to the decomposition of CaP nanolids in the acidic lysomomal compartments; (b) At 48 h, most of the DOX resided in the nuclei for cells treated with CNT-GSH-G4-CaP-DOX, suggesting the efficient release of DOX from CNT-GSH-G4-CaP-DOX. Cells were imaged using a 100Xoil-immersion objective.

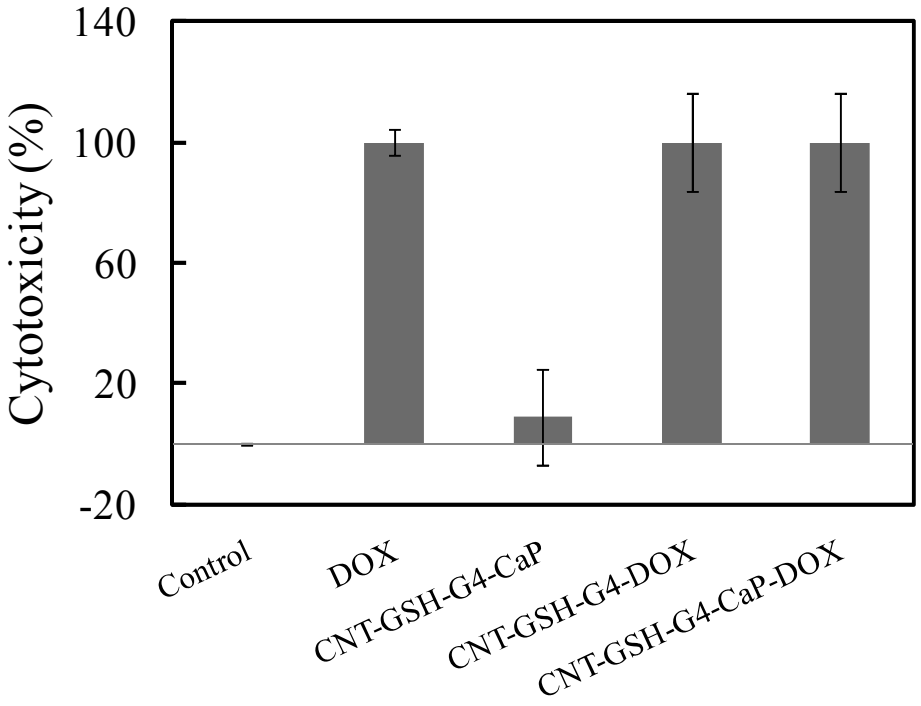

Fig. 9. Cytotoxicity analysis of nanosystems incubated for 48 h with HCT116 cells.

Table of Content

A pH-responsive carbon nanotube based carrier crowned with pore-blocking calcium phosphate nanopsule (CaP) is developed by dendrimer template technique. Upon exposure to cellular acidic lysosomal pH, guest anticancer drug is released from carbon nanotube due to pore uncapping by decomposition of CaP nanolids.